

# Circulation Research

JOURNAL OF THE AMERICAN HEART ASSOCIATION

American Heart  
Association®   
*Learn and Live*<sup>SM</sup>

## **Alterations in left ventricular mechanics, energetics, and contractile reserve in experimental heart failure**

MR Wolff, PP de Tombe, Y Harasawa, D Burkhoff, S Bier, WC Hunter, G Gerstenblith and DA Kass

*Circ. Res.* 1992;70;516-529

Circulation Research is published by the American Heart Association, 7272 Greenville Avenue, Dallas, TX 75214

Copyright © 1992 American Heart Association. All rights reserved. Print ISSN: 0009-7330. Online ISSN: 1524-4571

The online version of this article, along with updated information and services, is located on the World Wide Web at:

<http://circres.ahajournals.org>

Subscriptions: Information about subscribing to Circulation Research is online at  
<http://circres.ahajournals.org/subscriptions/>

Permissions: Permissions & Rights Desk, Lippincott Williams & Wilkins, a division of Wolters Kluwer Health, 351 West Camden Street, Baltimore, MD 21202-2436. Phone: 410-528-4050. Fax: 410-528-8550. E-mail:  
[journalpermissions@lww.com](mailto:journalpermissions@lww.com)

Reprints: Information about reprints can be found online at  
<http://www.lww.com/reprints>

# Alterations in Left Ventricular Mechanics, Energetics, and Contractile Reserve in Experimental Heart Failure

Matthew R. Wolff, Pieter P. de Tombe, Yasuhiko Harasawa, Daniel Burkhoff, Seth Bier, William C. Hunter, Gary Gerstenblith, and David A. Kass

The contributions of changes in primary systolic and diastolic properties, limitations of contractile reserve, and alterations in energy efficiency to the left ventricular dysfunction seen with chronic pacing tachycardia were investigated. Seven dogs (heart failure group) were ventricularly paced at 250 beats per minute for  $26.3 \pm 2.9$  days and compared with a separate control group ( $n=8$ ). Studies were performed with isolated, metabolically supported hearts coupled to a computer-controlled loading system. Pressure–volume relations and myocardial oxygen consumption ( $MVO_2$ ) were measured to assess chamber systolic and diastolic properties and efficiency (relation between  $MVO_2$  and pressure–volume area [PVA]). Systolic function was reduced in failure hearts versus controls as assessed by the slope of the end-systolic pressure–volume relation ( $1.29 \pm 0.94$  versus  $2.71 \pm 0.98$  mm Hg/ml,  $p < 0.01$ ) and lowered end-systolic stiffness at a matched stress ( $956.1 \pm 123.5$  versus  $1,401.7 \pm 431.7$  g/cm<sup>2</sup>,  $p < 0.05$ ). Diastolic chamber and myocardial stiffness were unaltered in failure hearts, but the unstressed diastolic-arrested volume was significantly larger ( $33.3 \pm 3.9$  versus  $21.9 \pm 7.6$  ml,  $p < 0.01$ ). Inotropic response to increased heart rate and exogenous  $\beta$ -adrenergic stimulation (dobutamine HCl) was significantly impaired in failure compared with control hearts. Most interestingly, failure hearts had a lowered slope of the  $MVO_2$ –PVA relation ( $2.1 \pm 1.1$  versus  $2.9 \pm 1.4$  ml O<sub>2</sub> · mm Hg<sup>-1</sup> · ml<sup>-1</sup> · 100 g left ventricle<sup>-1</sup>,  $p < 0.001$ ), indicating increased efficiency of chemomechanical energy conversion. The y intercept of the  $MVO_2$ –PVA relation, which reflects oxygen costs of basal metabolism and excitation–contraction coupling, was unchanged in the two groups despite decreased contractility of the heart failure hearts. These results demonstrate reduced chamber and myocardial contractility, dilatation without alteration of passive myocardial properties, impaired contractile reserve, and novel alterations in cardiac efficiency in this model of heart failure. (*Circulation Research* 1992;70:516–529)

**KEY WORDS** • pressure–volume relations • cardiomyopathy • force–frequency •  $\beta$ -adrenergic receptors • pacing tachycardia • diastole • contractility • canine heart failure model

**R**apid pacing over a period of several weeks leads to ventricular dilation, decreased fractional shortening, elevated filling pressures, and congestive heart failure in several animal species.<sup>1–5</sup> Prior studies have revealed neurohumoral changes in this model similar to those observed in human congestive heart failure.<sup>6,7</sup> Evidence of myocardial dysfunction in patients with persistent tachyarrhythmias suggests that this model may share some characteristics with human dilated cardiomyopathies.<sup>8</sup> Although prior animal studies have clearly demonstrated reduced ventricular pump

performance from chronic rapid pacing, the mechanisms underlying this dysfunction remain poorly characterized. There are several mechanisms definable at a chamber level that could contribute to reduced net pump function. These include 1) primary reductions in chamber and/or myocardial contractility, 2) abnormal diastolic chamber and/or myocardial stiffness, 3) reduced inotropic reserve caused by blunting of the positive force–frequency relation or decreased response to  $\beta$ -adrenergic stimulation, and 4) a reduced ability to convert consumed oxygen to mechanical work (decreased metabolic efficiency). The purpose of the present study was to determine the contribution of each of these factors to the cardiac failure induced by chronic rapid pacing.

To elucidate the role of each of these mechanisms, studies were performed using isolated, metabolically supported canine hearts coupled to a computer-simulated vascular loading system. This preparation offers the advantages of rigid control of chamber load, heart rate, and coronary perfusion and precise measurements of ventricular volume and myocardial oxygen consumption ( $MVO_2$ ). The results demonstrate reductions in chamber and myocardial contractility, ventricular dila-

From the Division of Cardiology, Department of Medicine (M.R.W., D.B., S.B., G.G., D.A.K.) and Department of Biomedical Engineering (P.P. de T., Y.H., W.C.H.), The Johns Hopkins Medical Institutions, Baltimore, Md.

Supported by National Heart, Lung, and Blood Institute (NHLBI) Ischemic Heart Disease SCOR HL-17655, NHLBI HL-18912, NHLBI Physician Scientist Award HL-01820 (D.A.K.), and American Heart Association (Maryland Affiliate) training grants (P.P. de T. and D.B.). D.A.K. is an Established Investigator of the American Heart Association.

Address for correspondence: David A. Kass, MD, Division of Cardiology, Carnegie 538, Johns Hopkins Hospital, 601 North Wolfe Street, Baltimore, MD 21205.

Received April 12, 1991; accepted October 31, 1991.

tation without alterations in passive myocardial stiffness, and impairment of contractile reserve via the force–frequency relation and  $\beta$ -adrenergic stimulation. In addition, evidence for alterations in metabolic efficiency in this form of heart failure is provided.

### Materials and Methods

Congestive heart failure was produced in seven adult mongrel dogs (mean weight,  $25.3 \pm 1.9$  kg) by chronic rapid right ventricular pacing for 4 weeks or until signs of congestive heart failure were clinically apparent (mean,  $26.3 \pm 2.9$  days). An additional eight healthy adult mongrel dogs (mean weight,  $24.7 \pm 1.1$  kg) were used as controls.

#### *Surgical Preparation*

Dogs were anesthetized with pentobarbital sodium (30 mg/kg i.v.). A 7F balloon-tipped catheter was introduced into the left jugular vein and advanced into the main pulmonary artery. Right atrial, right ventricular, pulmonary artery, and capillary wedge pressures were obtained. The catheter was removed, and a bipolar screw-in endocardial pacing electrode was advanced to the right ventricular apex under fluoroscopic guidance. The lead was tunneled to a subcutaneous pocket in the left lateral neck and connected to a pulse generator (model SX 5984 or 5940, Medtronic, Inc., Minneapolis, Minn.), modified to pace rapidly by gluing a magnet to the canister, which disabled the rate limit. Animals were allowed to recover, and 1 or 2 days after pacemaker implantation a two-dimensional short-axis echocardiogram was obtained at the level of the papillary muscle heads. The pacemaker was then programmed to 250 beats per minute, and animals were examined daily for evidence of pulmonary and right heart congestion (ascites). Repeat echocardiography was performed after 2 weeks of pacing and 1–2 days before the isolated heart study. All echocardiograms were obtained with pacing temporarily suspended. Endocardial short-axis contours from at least three beats were averaged to determine end-diastolic (maximal) and end-systolic (minimal) areas and area ejection fraction.

#### *Isolated Heart Preparation*

Details of the blood-perfused isolated canine heart preparation have been previously reported.<sup>9</sup> Briefly, a support dog (weight, 25–30 kg) was anesthetized with pentobarbital sodium (30 mg/kg i.v.), heparinized (5,000 units i.v.), and mechanically ventilated. The femoral arteries and veins were cannulated and connected to a perfusion system used to supply oxygenated blood to the isolated heart. The temperature of the perfusate was maintained at approximately 37°C with a heat exchanger. A donor animal from either the heart failure or control group was anesthetized with fentanyl citrate (10  $\mu$ g/kg i.v.) and pentobarbital sodium (10–20 mg/kg i.v.). Blood pressure was frequently supported with epinephrine (0.1–10  $\mu$ g/kg/min) during initial induction in the heart failure dogs. A 7F balloon-tipped catheter was advanced into the pulmonary artery, and right heart pressures were measured. In all but two cases, heart failure dogs were weaned from epinephrine before these hemodynamic measurements were obtained.

After right heart catheterization, the dog was mechanically ventilated and the chest opened via midline

sternotomy. The left subclavian artery was cannulated with the arterial perfusion line from the support dog and the heart isolated and removed. The left atrium was incised, the chordae tendineae cut from the mitral leaflets, and a metal adapter ring sutured onto the mitral annulus. A water-filled latex balloon, connected to a computer-controlled servo-pump system, was placed through the adapter into the left ventricular cavity. A small cannula inserted through the left ventricular apex was connected to negative pressure to drain thebesian blood flow and ensure close approximation between balloon and endocardium. Left ventricular (LV) pressure was measured by a micromanometer-tipped catheter (PC-380, Millar Instruments, Houston, Tex.) placed inside the latex balloon. Coronary sinus blood was drained from the right ventricle through an in-line ultrasonic flowmeter (Transonics, Ithaca, N.Y.) to measure coronary blood flow. The difference between arterial and coronary venous blood oxygen content was measured continuously by absorption spectrometry (A-VOX System) calibrated to a Lex-O<sub>2</sub>-Con oxygen analyzer. Electrodes were sutured to the ventricular surface and atrium for an electrocardiogram and pacing, respectively. Hearts were paced at 171 beats per minute (cycle length, 350 msec) during data collection, a rate chosen to ensure overdriving the atrial rhythm even during dobutamine infusion.

Several measures were taken to stabilize the preparation and reduce fluctuations in sympathetic outflow from the support dog. First, pentobarbital sodium (2–3 mg/kg/hr) was continuously infused to avoid fluctuations in the level of anesthesia. The support dog was premedicated with sodium hydrocortisone 500 mg i.m., diphenhydramine 25 mg i.m., and indomethacin 50 mg p.r. (likely minimizing release of platelet and white blood cell mediators during the extracorporeal circulation). Arterial and central venous pressures were continuously monitored and arterial pH, PO<sub>2</sub>, and PCO<sub>2</sub> determined every 30 minutes. Adjustments of ventilation rate, supplemental oxygen, correction of base deficits, and volume support were used when appropriate to maintain these parameters within normal ranges throughout the experiment. Finally, a two-pump perfusion system was used to maintain a constant hemodynamic load on the support dog. Arterial blood was pumped from the support dog at a constant rate (400–500 ml/min) irrespective of coronary flow in the isolated heart. A second pump shunted blood from the primary pump circuit back into the support dog, bypassing the isolated heart. This pump was servo-controlled to maintain a constant perfusion pressure (90 mm Hg) to the isolated heart.

LV volume was controlled by a servo-pump responding to a command signal generated by the computer solution of the cardiac interaction with a model vascular loading system (three-element Windkessel) as previously described in detail.<sup>9,10</sup> Windkessel parameters were arterial resistance (2.0 mm Hg · second · ml<sup>-1</sup>), characteristic impedance (0.3 mm Hg · second · ml<sup>-1</sup>), and compliance (0.4 ml · mm Hg<sup>-1</sup>), values similar to those derived from normal canine aortic impedance spectrum.<sup>11</sup> This loading system could also be changed to allow isovolumic contraction.

### Experimental Protocols

**Systolic and diastolic pressure–volume relations and energetics.** Steady-state data from ejecting beats were collected at five to six end-diastolic volumes, with end-diastolic pressure ranging from 0 to 20 mm Hg, to determine end-systolic pressure–volume relations (ESPVRs), end-diastolic pressure–volume relations (EDPVRs), and  $MVO_2$ . In each heart the volume intercept ( $V_o$ ) of the ESPVR was directly measured by reducing intraventricular volume until peak systolic pressure was zero.  $V_o$  measurements were reproducible to within 1 ml with multiple determinations.

**Force–frequency relation.** Heart rate was varied from 125 to 225 beats per minute. Because of a limited frequency response of the impedance loading system, these data were obtained isovolumically. Peak systolic pressure was determined at each heart rate.

**Dobutamine dose–response.** Dobutamine dose–response curves were obtained under ejecting conditions. Steady-state data were collected at baseline and with infusion of dobutamine into the isolated heart perfusion circuit at incremental rates (1, 5, 10, 20, 40, 80, 160, and 320  $\mu\text{g}/\text{min}$ ) up to the maximal tolerated rate, limited by arrhythmias and heart rate greater than 171 beats per minute. Because of practical limitations in obtaining data at multiple infusion rates, a single end-diastolic volume was used (chosen for each heart to produce an end-diastolic pressure of 8–12 mm Hg at baseline). Contractile response was indexed by steady-state stroke work. At the maximal dobutamine infusion rates, pressure–volume and energetic relations were also determined in the failure hearts by obtaining data at five or six randomly chosen end-diastolic volumes.

**Postmortem examination.** At the conclusion of the study the isolated heart was arrested in diastole by slow intracoronary infusion of saturated KCl solution. The heart was removed from the volume servo-system, atrial tissue resected, and the apical vent in the left ventricle closed by a purse-string suture. The left ventricle was then filled to the level of the mitral annulus with saline and submerged to that level in a saline bath. The intraventricular cavity was carefully aspirated. At least three such measurements were averaged to determine diastolic-arrested chamber volume at zero transmural pressure ( $V_{ref}$ ). Left ventricular (septum and free wall) and right ventricular free wall weights were also measured.

### Data Analysis

Data were recorded continuously on a strip-chart recorder (model 2800, Gould, Cleveland, Ohio) and also digitized at a rate of 500 Hz and stored on magnetic disk for off-line analysis. Data from five to 10 beats at each steady-state condition were signal averaged for analysis.

**Systolic pressure–volume relations.** Data obtained at multiple preload volumes were used to derive several systolic chamber function indexes. The ESPVR was derived from the points of maximal  $P/(V-V_o)$ . End-systolic points were fit to a linear elastance ( $E_{es}$ ) model

$$P_{es} = E_{es} \cdot (V_{es} - V_o) \quad (1)$$

where  $P_{es}$  is LV pressure at end systole and  $V_{es}$  is LV volume at end systole. Because in many cases the

ESPVR was obviously nonlinear, the end-systolic points were also fit to a parabolic relation

$$P_{es} = a \cdot (V_{es} - V_o) + b \cdot (V_{es} - V_o)^2 \quad (2)$$

where  $a$  is the slope of the ESPVR at  $V_o$ , and  $b$  is the coefficient of nonlinearity. The statistical significance of nonlinearity was determined by a Student's  $t$  test using the estimate and standard error of the estimate of the  $b$  coefficient. The null hypothesis ( $b=0$ , thus ESPVR is linear) was rejected if  $p < 0.05$  for the  $b$  term.

Because nonlinearity rendered statistical comparisons between ESPVRs somewhat difficult, two alternatives were used. One used the regression fits (linear or nonlinear) to estimate  $V_{es}$  at a common  $P_{es}$  (50 mm Hg), a larger  $V_{es}$  being consistent with decreased ventricular contractility. The second approach examined the relation between stroke work and end-diastolic volume. The slope of this linear relation is a load-insensitive measure of chamber contractility.<sup>12,13</sup>

**Diastolic pressure–volume relations.** End-diastolic points were fit to a monoexponential equation

$$P_{ed} = P_o + c \cdot (e^{dV_{ed}} - 1) \quad (3)$$

where  $P_{ed}$  and  $V_{ed}$  are end-diastolic pressure and volume, respectively,  $P_o$  is the pressure at  $V_o$ , and  $P_o$ ,  $c$ , and  $d$  are nonlinear fit parameters. Diastolic chamber stiffness ( $dP_{ed}/dV_{ed}$ ) was calculated from the first derivative of Equation 3. For comparisons between groups, diastolic chamber stiffness was determined at a common end-diastolic pressure (15 mm Hg).

**Stress–strain relations.** Systolic and diastolic pressure–volume relations have limitations in quantifying myocardial properties because of their dependence on chamber size and ventricular mass. Therefore a stress–strain analysis with a thick-walled spherical ventricular model was used (“Appendix”).

Both end-systolic and end-diastolic stress–strain relations were nonlinear and were fit well by monoexponential equations. In the case of the end-systolic relation, the equation was

$$\sigma_{es} = A \cdot (e^{B(\epsilon_{es} - \epsilon_o)} - 1) \quad (4)$$

where  $\sigma_{es}$  is end-systolic stress,  $\epsilon_{es}$  is end-systolic strain,  $\epsilon_o$  is the strain at  $V_o$ , and  $A$  and  $B$  are fit parameters. End-diastolic stress–strain relations were fit to the equation

$$\sigma_{ed} = C \cdot (e^{D\epsilon_{ed}} - 1) \quad (5)$$

where  $\sigma_{ed}$  is end-diastolic stress,  $\epsilon_{ed}$  is end-diastolic strain, and  $C$  and  $D$  are fit parameters. First derivatives of both stress equations with respect to strain were used to determine myocardial end-systolic and end-diastolic stiffness ( $d\sigma/d\epsilon$ ). For comparisons between heart groups, stiffness was determined at matched stresses (75 and 15  $\text{g}/\text{cm}^2$  for systole and diastole, respectively).

**Dobutamine dose–response.** The contractile response to  $\beta$ -adrenergic stimulation (dobutamine HCl) was assessed by change in stroke work with hearts ejecting against a fixed afterload impedance at a constant  $V_{ed}$  and heart rate. Intracoronary dobutamine concentration was calculated by dividing infusion rate by measured coronary blood flow. Because the relation between dobutamine concentration and stroke work did

not plateau in all hearts (particularly in the control group in which increased heart rate and arrhythmias limited the dobutamine infusion rate), data could not be meaningfully fit to the Hill equation. Instead, the relations were linearized using the logarithm of the dobutamine concentration, and multivariate linear regression analysis was used (see below) to compare the responses between animal groups.

**Myocardial energetics.** Ventricular energetics were characterized using the pressure–volume area (PVA)– $MVO_2$  relation framework described by Suga.<sup>14,15</sup> PVA is a measure of the total mechanical work performed by the left ventricle during a cardiac cycle and is defined as the area bound by the ESPVR, the EDPVR, and the systolic trajectory of the pressure–volume loop. The relation between  $MVO_2$  and PVA is linear in the normal isolated and in situ dog heart.<sup>15</sup> This framework allows partitioning of the  $MVO_2$  between oxygen consumption associated with ventricular work and non-work-related  $MVO_2$ . Hence, the efficiencies of these two aspects of myocardial energetics can be examined separately.

$MVO_2$  (per beat) was obtained as the difference between arterial and coronary venous blood oxygen content  $\times$  coronary blood flow/heart rate, neglecting the small amount of LV thebesian flow. LV  $MVO_2$  was calculated as suggested by Suga et al,<sup>15</sup> by subtracting estimated unloaded right ventricular oxygen consumption from the total  $MVO_2$ . LV  $MVO_2$  was expressed per beat and was normalized to 100 g LV.

PVA was determined by digitally integrating under the pressure–volume loop from end diastole to end systole and adding the area under the ESPVR between end systole and  $V_0$  (obtained by analytic integration of Equation 1 or 2). The area under the diastolic pressure–volume curve (EDPVR) between  $V_{ed}$  and the zero pressure intercept (obtained by analytic integration of Equation 3) was subtracted from the sum of the two previous areas. The small portion of PVA below the volume axis was not included in the calculated PVA. PVA was also normalized to 100 g LV weight.

### Statistical Methods

We used a multivariate linear regression model to compare  $MVO_2$ –PVA relations as well as other linear relations by using a dummy variable to represent the presence or absence of heart failure and additional dummy variables for each dog to adjust for interanimal variation.<sup>16</sup> Changes in echocardiographic parameters were tested with analysis of variance (ANOVA). Comparisons of other variables were made by two-tailed *t* tests. Differences were accepted as statistically significant for  $p < 0.05$ . All data are expressed as mean  $\pm$  SD unless otherwise specified. Statistical tests and nonlinear curve fitting were performed with commercially available software (SYSTAT, Inc., Evanston, Ill.).

### Results

Thirteen dogs were instrumented and underwent rapid ventricular pacing. Three animals died suddenly during the pacing period and two died during induction of anesthesia for the isolated heart study. A sixth dog was excluded because of pacer lead migration and extended interruption of pacing. The seven remaining dogs made up the heart failure group and were paced

**TABLE 1. Serial Echocardiographic Measurements From Failure Hearts**

	Prepacing	Pacing for 2 weeks	Pacing for 3 weeks
End-diastolic area (cm <sup>2</sup> )	12.2 $\pm$ 2.9	20.6 $\pm$ 4.7	22.8 $\pm$ 4.5*
End-systolic area (cm <sup>2</sup> )	7.5 $\pm$ 4.5	15.0 $\pm$ 2.8	17.7 $\pm$ 4.0*
Area ejection fraction	0.41 $\pm$ 0.13	0.26 $\pm$ 0.06	0.22 $\pm$ 0.05*

Short-axis cross-sectional echocardiographic areas were obtained from conscious animals with pacemaker off.

\* $p < 0.01$  vs. prepacing.

for an average of 26.3 $\pm$ 2.9 days. At the time of the isolated heart study, five dogs had clinical signs of congestive heart failure including anorexia, lethargy, ascites, and/or dyspnea. There was no significant change in body weight in the heart failure group over the pacing period.

Echocardiographic data from the heart failure dogs are provided in Table 1. Chronic rapid pacing led to increases in end-diastolic and end-systolic area of 86% and 136%, respectively, while area ejection fraction fell by 46%. Pulmonary capillary wedge pressure increased significantly over the pacing period (4.9 $\pm$ 2.7 versus 24.9 $\pm$ 5.1 mm Hg,  $p < 0.01$ ) as did right atrial pressure (2.4 $\pm$ 2.4 versus 15.7 $\pm$ 4.1 mm Hg,  $p < 0.01$ ). These echocardiographic and hemodynamic changes are similar to those previously reported for chronic rapid pacing in dogs using comparable pacing rate and duration.<sup>4,5</sup>

Postmortem data are provided in Table 2. Despite the increased chamber volume there were no differences in LV or right ventricular mass between heart failure and control animals or in the ratio of these weights to (prepacing) body weight. However, the volume of the KCl-arrested hearts at zero transmural pressure,  $V_{ref}$ , was significantly larger in the heart failure group (33.3 $\pm$ 3.9 versus 21.9 $\pm$ 7.6 ml in the control group,  $p < 0.01$ ), indicating a rightward shift in the passive (diastolic) pressure–volume relation.

### Systolic Ventricular Mechanics

Chronic rapid pacing reduced LV chamber contractility. Representative pressure–volume loops and corresponding ESPVRs and EDPVRs for a control (panel A) and heart failure (panel B) heart are shown in Figure 1. Despite some nonlinearity, end-systolic pressure–volume data were well fit by a linear regression (evidenced by average values of  $r^2 = 0.960$  and 0.983). On average, the slope of the ESPVR (end-systolic elastance or  $E_{es}$ )

**TABLE 2. Postmortem Weights and KCl-Arrested Diastolic Volumes Measured at Zero Transmural Pressure**

	Control	Heart failure
LV (g)	130.5 $\pm$ 17.0	119.9 $\pm$ 22.9
RV (g)	52.1 $\pm$ 13.3	41.6 $\pm$ 11.1
LV/body wt (g/kg)	5.28 $\pm$ 0.71	4.73 $\pm$ 0.97
RV/body wt (g/kg)	2.11 $\pm$ 0.55	1.65 $\pm$ 0.42
$V_{ref}$ (ml)	21.9 $\pm$ 7.6	33.3 $\pm$ 3.9*

LV, left ventricle; RV, right ventricle;  $V_{ref}$ , KCl-arrested diastolic volume at zero transmural pressure.

\* $p < 0.01$  vs. control.

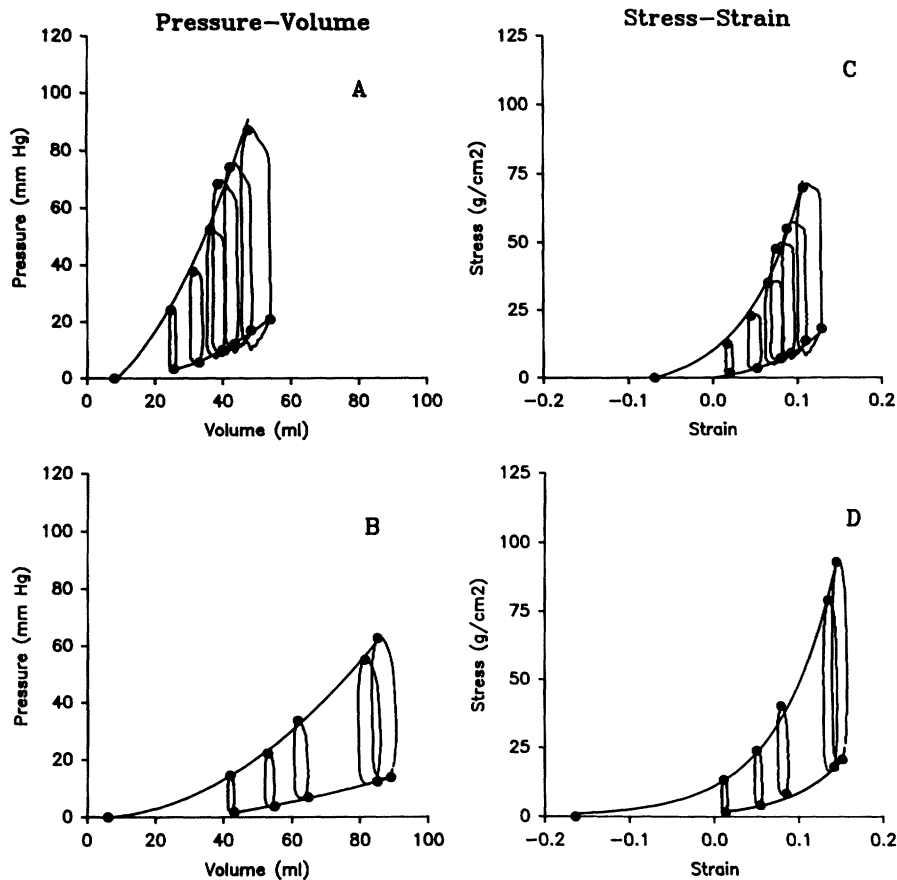


FIGURE 1. Pressure-volume and stress-strain loops for representative control (panels A and C) and failure (panels B and D) hearts.

was lower in heart failure ( $1.29 \pm 0.94$  mm Hg/ml) than in control ( $2.71 \pm 0.98$ ,  $p < 0.01$  by multivariate regression) hearts (Table 3). Nonlinear regression improved the ESPVR fit most notably in the failure hearts. End-systolic volume determined at a common end-systolic pressure (50 mm Hg) by using the best ESPVR fit revealed a higher volume in heart failure than control hearts ( $55.5 \pm 20.6$  versus  $27.1 \pm 9.8$  ml,  $p < 0.01$ ), also consistent with reduced chamber systolic function. Finally, the slope of the relation between stroke work and end-diastolic volume was significantly lower in the heart failure group than in controls ( $8.3 \pm 4.1$  versus  $29.3 \pm 9.7$  mm Hg,  $p < 0.01$ ).

Although the postmortem analysis revealed a significant increase in  $V_{ref}$  in the heart failure ventricles, an analogous shift in  $V_o$ , the volume intercept of the ESPVR, did not occur (Table 3).  $V_o$  for the failure hearts ( $6.4 \pm 2.9$  ml) was virtually the same as for the control hearts ( $5.1 \pm 2.2$  ml,  $p = \text{NS}$ ).

Because the preceding indexes of systolic function are based on chamber pressure-volume data, they are dependent on ventricular geometry and mass as well as intrinsic myocardial properties. To examine myocardial systolic function, a stress-strain analysis was used. Stress-strain loops for the same representative hearts are provided in Figures 1C and 1D. In all cases, the end-systolic stress-strain relations were well fit by a monoexponential model. Relations were compared using end-systolic myocardial stiffness calculated at a common end-systolic stress ( $75$  g/cm<sup>2</sup>), which was significantly less in heart failure than controls ( $956.1 \pm 123.5$  versus  $1,401.3 \pm 431.7$  g/cm<sup>2</sup>,  $p < 0.05$ ). This differ-

ence suggests decreased myocardial contractility in the heart failure ventricles. Similar results were obtained using a common end-systolic stress of 50 or 100 g/cm<sup>2</sup>. Average end-systolic stress-strain relations in the two groups, obtained by calculating strains at common stresses, are shown in Figure 2.

#### Diastolic Ventricular Mechanics

As previously noted, chronic pacing tachycardia induced an increase in the unstressed diastolic volume,  $V_{ref}$ , of nearly 50% over controls (Table 2), suggesting chamber remodeling. Diastolic chamber stiffness, calculated as the slope of the EDPVR at a common end-diastolic pressure (15 mm Hg), was similar in the two groups ( $1.00 \pm 0.71$  control versus  $0.68 \pm 0.19$  mm Hg/ml heart failure,  $p = \text{NS}$ ), although interanimal variability was considerable. End-diastolic myocardial stiffness calculated at a common end-diastolic stress (15 g/cm<sup>2</sup>) was also similar in the two groups ( $325.0 \pm 170.5$  control versus  $291.9 \pm 72.1$  g/cm<sup>2</sup> heart failure,  $p = \text{NS}$ ). Comparison of end-diastolic stiffness at a common end-diastolic stress of 10 or 20 g/cm<sup>2</sup> also showed no difference between groups. Average end-diastolic stress-strain relations for the two groups, obtained by calculating strains at common end-diastolic stresses, are also shown in Figure 2 and suggest no alteration of passive diastolic myocardial properties.

#### Force-Frequency Relation

In normal canine ventricles, increases in heart rate are associated with increases in contractility.<sup>17</sup> To test

TABLE 3. End-systolic Pressure–Volume Relations From Control and Failure Hearts

Dog	V <sub>o</sub>	Linear fit		Quadratic fit				V <sub>50</sub>
		E <sub>es</sub>	r <sup>2</sup>	a	b	p	r <sup>2</sup>	
Control								
1	5	2.1±0.1	0.992	1.0±0.2	0.023±0.194	<0.01	0.999	34.2
2	8	2.0±0.1	0.974	0.8±0.4	0.040±0.012	<0.05	0.992	35.2
3	7	4.0±0.5	0.930	...#	...	NS	...	19.6
4	6	1.3±0.1	0.963	0.1±0.2	0.029±0.003	<0.001	0.998	45.1
5	2	2.6±0.3	0.930	...	...	NS	...	21.2
6	6	4.1±0.4	0.960	...	...	NS	...	18.3
7	2	2.4±0.2	0.960	...	...	NS	...	22.7
8	5	3.2±0.3	0.968	...	...	NS	...	20.2
Mean	5.1	2.71	0.960					27.1
SD	2.2	0.98	...					9.8
Heart failure								
9	5	1.2±0.1	0.993	*	*	NS	*	47.6
10	6	0.7±0.1	0.964	0.1±0.1	0.009±0.001	<0.001	0.999	77.5
11	5	0.6±0.1	0.996	0.1±0.1	0.010±0.001	<0.001	0.997	73.3
12	12	1.0±0.1	0.992	0.5±0.2	0.011±0.003	<0.05	0.993	61.3
13	6	0.7±0.1	0.975	0.3±0.1	0.009±0.001	<0.05	0.998	65.5
14	8	1.5±0.1	0.978	0.9±0.2	0.012±0.004	<0.05	0.992	44.6
15	3	3.3±0.2	0.980	...	...	NS	...	18.0
Mean	6.4	1.29*	0.983					55.5†
SD	2.9	0.94	...					20.6
Heart failure (maximal dobutamine stimulation)								
9	5	1.7±0.1	0.983	...	...	NS	...	34.0
10	6	1.2±0.1	0.985	...	...	NS	...	47.4
11	5	0.9±0.1	0.959	...	...	NS	...	62.9
12	12	2.6±0.0	0.999	...	...	NS	...	31.6
13	6	1.5±0.1	0.986	0.9±0.2	0.014±0.004	<0.05	0.997	42.6
14	8	3.5±0.2	0.978	...	...	NS	...	22.5
15	3	11.2±1.1	0.957	...	...	NS	...	7.5
Mean	6.4	3.23‡	0.980					35.5†
SD	2.9	3.63	...					17.9

For linear fit, P<sub>es</sub>=E<sub>es</sub>×(V<sub>es</sub>−V<sub>o</sub>), where P<sub>es</sub> is end-systolic pressure, E<sub>es</sub> is end-systolic elastance, V<sub>es</sub> is end-systolic volume, and V<sub>o</sub> is the volume intercept. For quadratic fit, P<sub>es</sub>=a×(V<sub>es</sub>−V<sub>o</sub>)+b×(V<sub>es</sub>−V<sub>o</sub>)<sup>2</sup>. p is statistical significance of nonlinearity. V<sub>50</sub> is the end-diastolic volume at P<sub>es</sub>=50 mm Hg. V<sub>o</sub> and V<sub>50</sub> are given in milliliters, E<sub>es</sub> and a in mm Hg/ml, and b in mm Hg/ml<sup>2</sup> (see “Materials and Methods”).

\*p<0.001 compared with control (multivariate regression analysis).

†p<0.01 compared with control (t test).

‡p<0.001 compared with heart failure baseline (multivariate regression analysis).

#Quadratic fit parameters are not shown if p>0.05 for nonlinear coefficient (b).

whether this force–frequency relation was altered by chronic pacing tachycardia, peak systolic (end-systolic) pressure of isovolumic contractions was determined at incremental heart rates. Minimum heart rate was limited by the spontaneous heart rate of the preparation, typically between 100 and 125 beats per minute, while maximum heart rate was limited by the development of mechanical alternans at rates greater than 225 beats per minute. Peak systolic pressure at each heart rate was normalized to the peak systolic pressure at 125 beats per minute (Figure 3). Although the controls demonstrated a positive rate treppe characteristic of most mammalian cardiac muscle (+1.8×10<sup>−3</sup>×HR+0.77, where HR is heart rate; multiple r<sup>2</sup>=0.842, p<0.01 for slope not

equal to zero), this relation was flat for the heart failure group (−0.47×10<sup>−3</sup>×HR+1.08; r<sup>2</sup>=0.70, slope not significantly different from zero).

### β-Adrenergic Responsiveness

To determine whether chronic pacing tachycardia alters the magnitude of the contractile response to β-adrenergic stimulation, dobutamine was infused into the perfusion circuit in incremental doses. Inotropic response was assessed by stroke work at a fixed end-diastolic volume, afterload, and heart rate. Figure 4 shows dobutamine response relations for control and heart failure dogs (data from one control heart could not be obtained because of

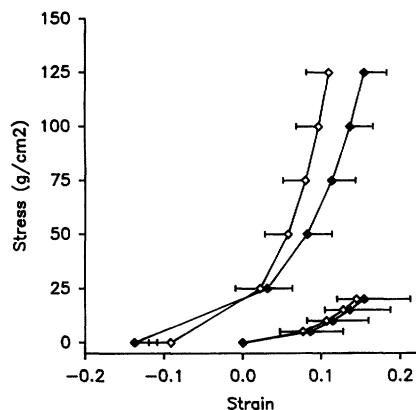


FIGURE 2. Average end-systolic (upper curves) and end-diastolic (lower curves) stress-strain relations for the control (open diamonds) and heart failure (closed diamonds) groups. Points were calculated at common end-systolic or end-diastolic stresses for each heart by using fitted end-systolic and end-diastolic stress-strain relations (see "Materials and Methods"). Error bars are  $\pm$ SD.

severe arrhythmias during dobutamine infusion). Panel A shows a representative example, and panel B shows the same data normalized to baseline and plotted on a semi-logarithmic scale. Normalized responses for the group data are provided in panel C. There was a marked reduction in the contractile response to dobutamine in the heart failure group ( $p < 0.001$  by multivariate regression analysis).

At the maximally tolerated dobutamine infusion rates, data were again collected in failure hearts at varying preloads to obtain complete pressure-volume relations. With this high level of  $\beta$ -adrenergic stimulation,  $E_{es}$  increased to levels comparable to the control group at baseline (Table 3). Interestingly, the ESPVRs also became more linear at this inotropic state. At

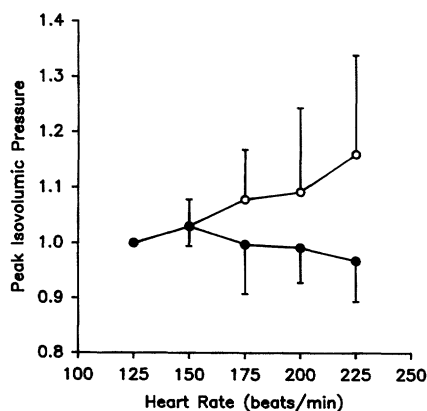


FIGURE 3. Force-frequency relations for control (open circles) and heart failure (closed circles) groups. Maximum isovolumic pressure has been normalized to the initial value (125 beats per minute). The slope of the two relations differ by multivariate regression analysis ( $p < 0.01$ ). Whereas the slope of the relation between heart rate and normalized peak pressure is positive for controls ( $p < 0.01$ ), the slope of this relation does not significantly differ from zero for the failure hearts. Error bars are  $\pm$ SD.

baseline, two of seven ESPVRs from the heart failure group were linear, whereas with dobutamine stimulation, six of seven ESPVRs in the heart failure group were linear ( $p < 0.05$  by  $\chi^2$  test).

Because failure but not control hearts were exposed to epinephrine during induction of anesthesia and donor heart isolation (see "Materials and Methods"), it is possible that the blunted dobutamine dose-response in the heart failure group was due to acute  $\beta$ -adrenergic downregulation. This hypothesis was tested in three additional controls that received epinephrine (1–2  $\mu$ g/kg/min, raising systolic blood pressure to greater than 200 mm Hg) during the entire heart isolation procedure. The results shown in Figure 4C (filled triangles) did not differ from the other control data.

Another potential mechanism for the blunted inotropic response in failure hearts to exogenous catecholamines is limited coronary flow reserve. In the isolated heart preparation coronary perfusion pressure is held constant; the primary determinant of coronary blood flow was PVA. Measured coronary blood flow and PVA from both experimental groups, averaged over common PVAs, are shown in Figure 5. Considerable coronary flow reserve exists in both experimental groups, because coronary flow increased by over 100% during dobutamine infusion. Coronary blood flow increased from  $82.2 \pm 29.7$  ml/min/100 g at baseline to  $168.6 \pm 34.1$  ml/min/100 g at the maximal tolerated dobutamine dose in the control hearts. In the heart failure group, coronary blood flow similarly increased from  $78.4 \pm 18.4$  ml/min/100 g at baseline to  $158.6 \pm 39.6$  at maximally tolerated dobutamine doses ( $p = \text{NS}$  versus controls at baseline and at maximal dobutamine dose). Individual coronary blood flow-PVA relations in both groups did not demonstrate a plateau, suggesting that total coronary flow reserve was not exhausted in either group during dobutamine infusion.

#### Myocardial Energetics

To test for alterations in metabolic efficiency in the failing ventricles,  $MVO_2$ -PVA relations were obtained and compared with those of controls. Figure 6 (upper panel) shows representative  $MVO_2$ -PVA relations for control and failure hearts.  $MVO_2$ -PVA relations were highly linear in both groups, and individual regressions are provided in Table 4 ( $MVO_2$ -PVA data could not be obtained from one control heart because of technical problems). There was a significant difference in the slope of the  $MVO_2$ -PVA relations between control and failure hearts ( $2.88 \times 10^{-5}$  versus  $2.10 \times 10^{-5}$  ml  $O_2 \cdot \text{mm Hg}^{-1} \cdot \text{ml}^{-1}$ ,  $p < 0.001$ ). Averaged  $MVO_2$ -PVA relations for the two groups, obtained by multivariate regression analysis, are provided in Figure 6 (lower panel).

Because PVA is theoretically an expression of mechanical energy, the ratio of PVA to  $MVO_2$  in excess of unloaded  $MVO_2$  (or the inverse of the slope of the  $MVO_2$ -PVA relation) reflects the efficiency of chemo-mechanical energy transduction.<sup>15</sup> When both  $MVO_2$  and PVA are expressed in joules per beat per 100 g  $LV^{-1}$ , this ratio is dimensionless. The mean slope values of the  $MVO_2$ -PVA relations from this study correspond to mean chemo-mechanical transduction efficiencies of 23% in the control group versus 32% in failure hearts.

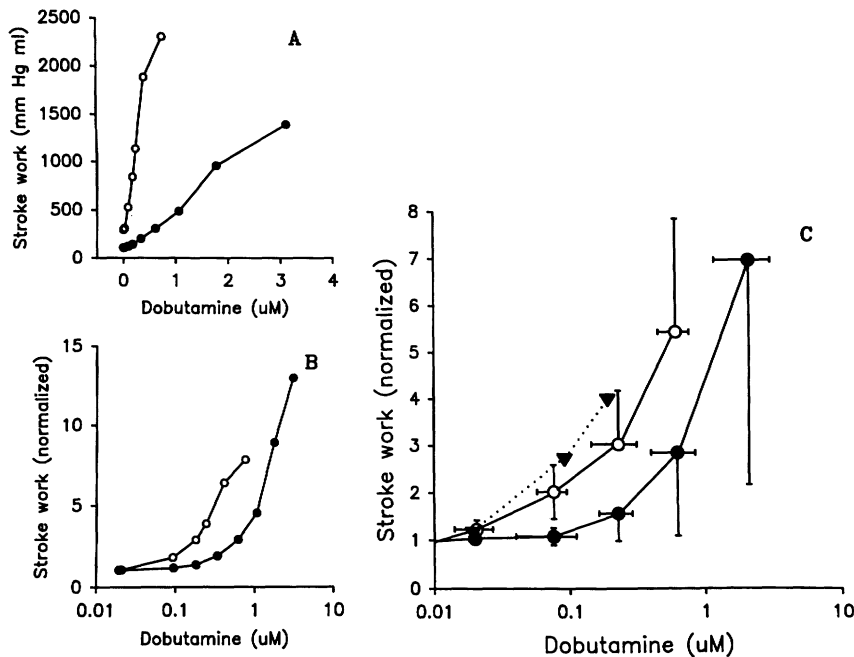


FIGURE 4. Inotropic response to intracoronary dobutamine infusion. Panel A: Responses of stroke work (obtained with fixed preload, afterload, and heart rate) in representative control (open circles) and failure (closed circles) hearts. Panel B: The same data plotted on a semilogarithmic scale, with stroke work normalized to the baseline value. Panel C: Average responses for control (open circles) and heart failure (closed circles) groups. Data are presented as mean  $\pm$  SD (on both axes), grouped by common concentrations. The two group responses differ by multivariate regression analysis ( $p < 0.001$ ). Filled triangles represent the means from three additional control hearts, all treated with epinephrine during the donor heart isolation procedure. These data points, also grouped by common concentrations, fall within the control group response (see text).

The y axis intercepts of the  $MVO_2$ -PVA relation (unloaded LV  $MVO_2$ ) were similar between control and failure hearts ( $0.030$  versus  $0.032$  ml  $O_2 \cdot \text{beat}^{-1} \cdot 100$  g  $LV^{-1}$ ,  $p = \text{NS}$ ), yet prior studies in canine hearts have shown unloaded  $MVO_2$  directly correlates with the contractile state ( $E_{es}$ ) of the ventricle,<sup>18,19</sup> and contractility was depressed in the failure hearts (Table 3). Thus, non-work-related oxygen costs were actually increased relative to contractile state in heart failure.  $MVO_2$ -PVA relations obtained from failure hearts during infusion of dobutamine further support this interpretation. Intracoronary dobutamine at maximally tolerated doses increased contractility and  $MVO_2$  in the failure hearts, resulting in a parallel upward shift in the  $MVO_2$ -PVA relation (Figure 6). Dobutamine enhanced  $E_{es}$  in the failure hearts to a level that was comparable to that of the control hearts.

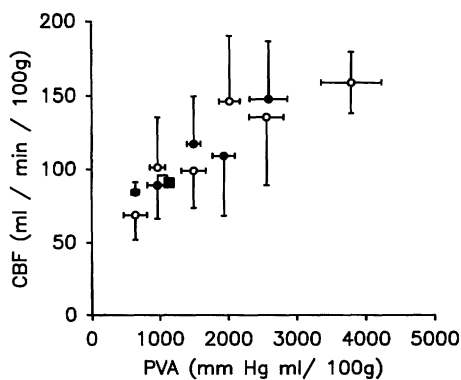


FIGURE 5. Coronary blood flow (CBF)-pressure-volume area (PVA) relations for the control (open circles) and heart failure (closed circles) groups as PVA was increased by incremental intracoronary dobutamine infusion. CBF-PVA data are grouped by common PVAs. Superimposed on these relations are the mean CBF-PVA points obtained at the highest end-diastolic volume in the absence of dobutamine (control, open square; failure, closed square).

The unloaded  $MVO_2$ , however, was significantly greater than control heart values ( $0.048 \pm 0.014$  dobutamine-stimulated heart failure versus  $0.032 \pm 0.009$  ml  $O_2 \cdot \text{beat}^{-1} \cdot 100$  g  $LV^{-1}$  control,  $p < 0.001$ ).

## Discussion

Chronic rapid ventricular pacing in dogs has been shown to induce clinical signs of congestive heart failure with ventricular dilatation, elevated cardiac filling pressures, and decreased fractional shortening.<sup>3-5</sup> Our results demonstrate chamber contractile depression and decreased myocardial end-systolic stiffness in this model of heart failure. An increased unstressed diastolic volume suggested chamber remodeling; however, no change was observed in diastolic stiffness or in the systolic volume at zero pressure. Failure hearts displayed blunted inotropic response to both increased heart rate and exogenous  $\beta$ -adrenergic stimulation. Lastly, we found novel changes in myomechanical energetics with increased efficiency of chemomechanical energy conversion and increased unloaded oxygen consumption relative to contractile state.

### Systolic Ventricular Mechanics

Several load-independent measures of chamber systolic function, assessed at constant coronary perfusion pressure and heart rate, were reduced in the heart failure group. The nonlinearity of the ESPVR (convex to the volume axis) observed in most failure hearts has not been previously described in models of chronic LV dysfunction. However, we have observed similar nonlinearities in both normal isolated<sup>20</sup> and in situ<sup>21</sup> canine hearts when contractility is acutely depressed pharmacologically. It would appear that the curvilinearity of the ESPVR observed in the failure hearts resulted from a contractility-dependent mechanism, since the ESPVRs became more linear with dobutamine stimulation.

An unexpected finding was that the volume intercept of the ESPVR was unchanged despite ventricular dila-

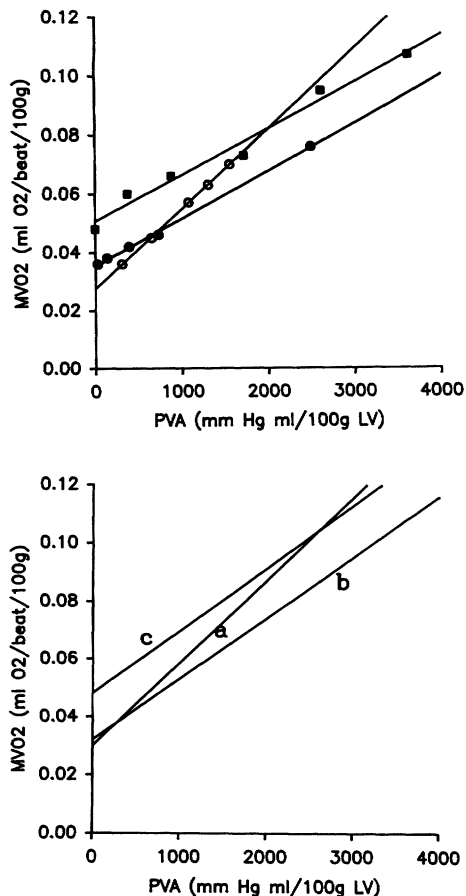


FIGURE 6. Upper panel: Myocardial oxygen consumption ( $MVO_2$ )–pressure–volume area (PVA) relations for representative control (open circles) and failure (closed circles) hearts.  $MVO_2$ –PVA points obtained in the heart failure example during maximum dobutamine infusion are also shown (closed squares). Lower panel: Average  $MVO_2$ –PVA relation for control (line a) and heart failure (line b) groups. Heart failure resulted in a significantly lower slope but did not alter the y intercept of the  $MVO_2$ –PVA relation relative to control. The average  $MVO_2$ –PVA relation for failure hearts during maximal dobutamine infusion is represented by line c. Dobutamine increased the y intercept without altering the slope of the  $MVO_2$ –PVA relation relative to baseline. Individual and average regression coefficients as well as statistical comparisons are provided in Table 4.

tation. Previous studies in conscious humans with dilated cardiomyopathy,<sup>22,23</sup> isolated and metabolically supported cardiomyopathic human hearts,<sup>24</sup> and anesthetized dogs with chronic pressure or volume overload<sup>25</sup> have all reported an increase in  $V_o$  with cardiac dilatation. Why  $V_o$  was unchanged despite a rightward shift of the EDPVR (increased  $V_{ref}$ ) is unclear. It is possible that ventricular remodeling, by altering the manner in which shortening of individual muscle segments is translated into changes in LV volume, could explain this dissociation. Alternatively, an increase in the passive slack length of the sarcomere may underlie this phenomenon.

As a consequence of chamber dilatation without a commensurate increase in wall mass, systolic wall

stresses at comparable chamber pressures were greater in failure hearts than in controls. However, stress–strain analysis provided evidence for depression of intrinsic myocardial contractility. For this analysis we used a thick-walled spherical model of the ventricle to calculate circumferential stress and strain and assess myocardial contractility. The diastolic-arrested zero-pressure volume was chosen as the reference volume rather than  $V_o$ , because  $V_o$  was unchanged in the failure hearts despite ventricular dilatation. Using  $V_o$  as a reference volume would increase the strains relative to stresses in heart failure and so further increase the differences between the two groups. Because the complex geometry of the ventricle is only approximated by a thick-walled sphere, circumferential stresses may be underestimated by 20–40%.<sup>26</sup> However, a spherical model may be more appropriate for an isolated heart preparation, in which disruption of the mitral apparatus results in a more spherical LV geometry.<sup>27</sup>

#### Diastolic Ventricular Mechanics

Given the dramatic increase in echocardiographic dimensions produced by chronic rapid pacing, the rightward shift of the EDPVR was anticipated. What was surprising, however, was that passive diastolic myocardial properties, as indexed by the fitted end-diastolic stress–strain functions, did not differ between the two groups. This finding is intriguing because interstitial edema, fibrosis, and increase in collagen volume fraction have been demonstrated in this model,<sup>28</sup> although after a somewhat longer duration of pacing.

#### Contractile Reserve Mechanisms

Limitations of cardiac inotropic reserve can play a role in the development of heart failure. The present study tested two physiological mechanisms by which the heart increases inotropic state, the force–frequency relation and the response to exogenous  $\beta$ -adrenergic stimulation. In both cases, there was a significant blunting of the cardiac response over a broad range of heart rate and catecholamine concentration. Abnormalities of the force–frequency relation have been previously demonstrated in patients with dilated cardiomyopathy<sup>29</sup> and in isolated myocardium from similar patients.<sup>30</sup> Our study demonstrates a similar blunting of the force–frequency relation in pacing tachycardia cardiomyopathy. The mechanism of the positive force–frequency relation in normal myocardium is probably a rate-related increase in the intracellular systolic calcium transient,<sup>31</sup> and abnormalities in the force–frequency relation may imply abnormalities in intracellular calcium handling in this model.

Our finding of diminished response to  $\beta$ -adrenergic stimulation is consistent with recent preliminary data in conscious chronically paced dogs.<sup>32</sup> Chronic rapid ventricular pacing results in gradual increases in plasma epinephrine and norepinephrine<sup>7</sup> that might be expected to result in a desensitization of the myocardial  $\beta$ -adrenergic receptor complex. Several reports suggest that the majority of LV desensitization to  $\beta$ -adrenergic stimulation is due to reductions of adenylate cyclase activity rather than a reduction in  $\beta$ -receptor density.<sup>32,33</sup>

Analysis of the relation between total coronary blood flow and LV work argues against a role of limitations in

TABLE 4. Myocardial Oxygen Consumption and Pressure-Volume Area Relations From Individual Control and Failure Hearts

Dog	Slope (ml O <sub>2</sub> · mm Hg <sup>-1</sup> · ml <sup>-1</sup> · 10 <sup>-5</sup> )	MVO <sub>2</sub> intercept (ml O <sub>2</sub> · beat <sup>-1</sup> · 100 g LV <sup>-1</sup> )	r <sup>2</sup>
<b>Control</b>			
1	2.8	0.027	0.999
2	2.4	0.021	0.992
3	3.2	0.036	0.995
4	4.3	0.034	0.942
5	2.5	0.028	0.980
7	2.4	0.039	0.971
8	2.6	0.028	0.984
Mean	2.88	0.030	0.982
SD	1.41	0.006	...
<b>Heart failure</b>			
9	1.5	0.030	0.971
10	2.1	0.014	0.969
11	2.6	0.029	0.968
12	2.8	0.038	0.998
13	2.1	0.043	0.818
14	1.7	0.036	0.963
15	1.9	0.034	1.000
Mean	2.10*	0.032	0.975
SD	1.12	0.009	...
<b>Heart failure (dobutamine infusion)</b>			
9	2.1	0.038	0.897
10	2.4	0.025	0.996
11	2.7	0.034	0.979
12	2.0	0.067	0.980
13	3.0	0.067	0.989
14	1.6	0.051	0.979
15	2.1	0.047	0.998
Mean	2.16*	0.048†	0.986
SD	0.51	0.014	...

MVO<sub>2</sub>, myocardial oxygen consumption; LV, left ventricle.

\**p* < 0.001 compared with control.

†*p* < 0.001 compared with control and heart failure baseline.

coronary blood flow to the impaired inotropic reserve in heart failure. However, because systolic wall stresses at higher dobutamine concentrations were greater in the dilated hearts than in the controls, a contribution of subendocardial ischemia to the impaired  $\beta$ -adrenergic responsiveness cannot be excluded. However, prior studies have shown that subendocardial blood flow (measured by radiolabeled microspheres) is not altered by chronic rapid pacing in dogs, despite even higher in situ end-diastolic pressures than those used in the present study.<sup>34</sup> Furthermore, it is worth noting that end-diastolic pressures during both incremental pacing and dobutamine infusion did not change. Elevation of end-diastolic pressure has been associated with subendocardial ischemia in other experimental models.<sup>35-37</sup>

#### Myocardial Energetics

Perhaps the most intriguing result of the present study is the finding that the slope of the MVO<sub>2</sub>-PVA relation

was decreased with heart failure, suggesting an increase in the chemomechanical conversion efficiency of the failing ventricle. As previously noted, acute changes in myocardial contractility change the offset but not the slope of the MVO<sub>2</sub>-PVA relation.<sup>18,19</sup> Changes in the slope of the MVO<sub>2</sub>-PVA relation have been interpreted as reflecting alterations in myofibrillar energy efficiency.<sup>15</sup> Before this interpretation is discussed, however, several alternative explanations should also be considered. These include changes in metabolic substrate preference, an increased sensitivity of failure hearts to myocardial ischemia, and/or limitations of the MVO<sub>2</sub>-PVA framework in assessing myocardial energetics.

Numerous studies have suggested that metabolic substrate can alter myocardial efficiency and that free fatty acids increase MVO<sub>2</sub> as compared with glucose consumption.<sup>38,39</sup> Because free fatty acids are the preferred substrate of normal myocardium,<sup>40</sup> an increase in glucose

metabolism could favorably affect the efficiency of ATP synthesis in failing hearts. Recent studies have demonstrated increased glucose and decreased free fatty acid uptake in pressure-overloaded rat hearts.<sup>41,42</sup> However, Burkhoff et al<sup>43</sup> found that in crystalloid perfused rat hearts, hexanoate (a short-chain fatty acid) alters the  $MVO_2$ -PVA relation by increasing the  $y$  intercept but not the slope when compared with a glucose-containing perfusate. Also inconsistent with this hypothesis is our finding of an unchanged unloaded  $MVO_2$  in the failure hearts, which would be expected to decrease if the efficiency of ATP synthesis were improved.

Marked reductions in coronary perfusion pressure have been shown to decrease the slope of the  $MVO_2$ -PVA relation in the normal isolated canine heart.<sup>19</sup> This finding was not attributed to increased efficiency of the contractile apparatus but rather to load sensitivity of both basal metabolism and the oxygen costs of excitation-contraction coupling under conditions of myocardial ischemia. A similar mechanism could apply to the failing ventricle. However, total coronary blood flow at the highest end-diastolic volume in each heart was similar in the two groups ( $92.6 \pm 34.9$  control versus  $90.7 \pm 21.9$  ml/min/100 g heart failure,  $p=NS$ ) and was much less than measured coronary blood flow during intracoronary dobutamine infusion ( $168.6 \pm 34.1$  control versus  $158.8 \pm 39.6$  ml/min/100 g heart failure at maximal dobutamine doses). Also, the slope of the  $MVO_2$ -PVA relation was not altered by high doses of dobutamine, a situation that would likely exacerbate ischemia if already present under baseline conditions.

In the  $MVO_2$ -PVA framework,  $MVO_2$  is partitioned into unloaded  $MVO_2$  (the sum of the oxygen consumptions associated with basal metabolism and excitation-contraction coupling) and the  $MVO_2$  associated with mechanical work. This construction depends on the assumption that oxygen consumption associated with basal metabolism and excitation-contraction coupling is independent of LV volume. As mentioned above, this may not be true in the case of reduced coronary perfusion pressure. In addition, a length dependence of both the systolic calcium transient and basal metabolism have been demonstrated in isolated cardiac muscle.<sup>44,45</sup> Despite these potential problems, the assumption seems reasonable in normal blood-perfused canine hearts, in which the  $MVO_2$  of ejecting contractions from a high preload against a negligible afterload (resulting in a very small PVA) is nearly the same as the  $MVO_2$  of unloaded contractions.<sup>46</sup>

It is also possible that PVA does not provide an adequate measure of total mechanical energy produced by crossbridge cycling because it does not incorporate the energetic consequences of an internal resistance to ejection or the positive and negative effects of shortening on contractility.<sup>47</sup> These effects, however, likely account for only a small fraction of work-related oxygen consumption,<sup>15</sup> and the magnitude of the efficiency change seen in this study is probably too large to be accounted for by these factors.

Alterations in the slope of the  $MVO_2$ -PVA relation may reflect changes in myofibrillar efficiency.<sup>15</sup> Only hyperthyroidism in rabbits has been shown to chronically alter the slope of the  $MVO_2$ -PVA relation,<sup>48</sup> while many acute interventions alter the  $MVO_2$  intercept without altering the slope of the relation. Thyroid

hormone causes an increase in the myosin isoform  $V_1/V_3$  ratio in rabbit ventricles, and the increase in the slope of the  $MVO_2$ -PVA relation was attributed to the change in the myosin ATPase accompanying this shift. Although the  $V_3$  myosin isoform predominates in the canine heart and is not altered with chronic rapid pacing, myofibrillar  $Ca^{2+}$ -ATPase activity is decreased in vitro by 26%.<sup>49</sup> It is possible that chronic posttranslational modification of the myosin ATPase or alteration of another protein constituent of the myofilament could alter the efficiency of mechanical energy production and that this change could be adaptive to conditions of increased stress and limited energy supply.

It is unclear whether our finding of increased chemomechanical efficiency of the contractile apparatus can be extended to other models of congestive heart failure or to human cardiomyopathies. Both reduced<sup>50,51</sup> and normal<sup>52,53</sup> myosin ATPase activity are reported in human cardiomyopathic hearts, the discrepancy in part relating to different techniques used to assay enzyme activity. Alpert and Mulieri<sup>54</sup> reported increases in myothermal economy (the relation between the tension-dependent heat liberated with isometric contractions and the force-time integral of those contractions) in isolated papillary muscles from rabbits with pressure-overload hypertrophy. A similar increase in myothermal economy has recently been reported in myocardium obtained from patients with heart failure.<sup>55</sup> Myothermal economy is not equivalent to the efficiency of the contractile apparatus reported in this study because it has units of velocity, in contrast to the dimensionless efficiency of the contractile apparatus obtained from  $MVO_2$ -PVA relations. However, these findings raise the possibility that alterations of the myofibril exist in the failing human heart, affecting its chemomechanical efficiency.

The mean efficiency of chemomechanical energy transduction of the control hearts in this study is less than the 35–45% that has been frequently reported for the normal canine heart.<sup>15</sup> However, previous studies from our<sup>56</sup> and other<sup>57</sup> laboratories with an isolated, blood-perfused preparation have reported efficiencies of less than 30% for normal canine hearts. A similarly low efficiency has also been reported for in situ canine hearts.<sup>58</sup> Although there is no obvious explanation for the differences in efficiencies of normal hearts between these studies, it should be noted that the present experiments were performed using the identical instrumentation under the same conditions for the control and failure groups. Furthermore, the order in which control or failure animals were studied was random. Nevertheless, the marked variability in efficiency must be kept in mind for comparison of data among different studies.

The second major observation made regarding the  $MVO_2$ -PVA relation was that unloaded  $MVO_2$  (representing the oxygen costs of basal metabolism and excitation-contraction coupling) was similar in the heart failure and control groups. Given the positive relation between contractile state and the unloaded  $MVO_2$  previously demonstrated in the normal isolated canine heart,<sup>18,19</sup>  $MVO_2$  is thus increased relative to ventricular or myocardial contractility in heart failure. Consistent with this interpretation is the finding that increasing contractility with dobutamine to levels comparable to controls led to significantly higher unloaded  $MVO_2$  in the failing hearts. Increased

unloaded  $MVO_2$  at a given contractile state could result from greater oxygen costs of basal metabolism or excitation–contraction coupling in heart failure. The latter could result from altered stoichiometry of the sarcoplasmic reticulum  $Ca^{2+}$ -ATPase and/or a decreased sensitivity of the myofilaments to calcium, although these issues remain speculative.

It should be noted that the overall efficiency of the ventricle, the ratio of external (stroke) work to  $MVO_2$ , depends on contractile state and loading conditions as well as the  $MVO_2$ –PVA relation. Because the contractility of the isolated heart preparation is certainly less than in situ and because the loading conditions used in this study were somewhat arbitrary, our data cannot be used to predict the effects of rapid-pacing–induced heart failure on the overall cardiac efficiency (ratio of stroke work to  $MVO_2$ ) in conscious animals.

### Limitations

A potential limitation of this study is that the loading conditions at which the two groups were compared do not reflect in situ loading conditions. In particular, the range of end-diastolic pressures used did not overlap the measured in situ pulmonary wedge pressures in the anesthetized failure dogs. High end-diastolic pressures were avoided because some normal canine hearts demonstrate altered systolic behavior and more rapid deterioration of function when operating at end-diastolic pressures of 25 mm Hg or greater. DPVRs and stress–strain relations were determined up to pressures of  $17.7 \pm 6.4$  mm Hg in control and  $18.6 \pm 6.7$  mm Hg in failure hearts, a range that should be sufficient to allow meaningful comparisons of the two groups. Also, the heart rate at which the study was performed (171 beats per minute) may have magnified differences between the two groups, because the force–frequency relation clearly differs at higher heart rates. This rate was chosen to allow data collection at a constant heart rate, even during dobutamine stimulation, and the effects of differences in the force–frequency relation were relatively small. Finally, afterload impedance for ejecting beats was identical for the two groups although aortic input impedance likely differs in situ. Although we did not attempt to duplicate in situ vascular physiology, an identical afterload allowed more direct comparisons of ventricular properties.

### Summary

The present study demonstrates several important features of chronic pacing tachycardia-induced heart failure. Reduction of systolic chamber function was confirmed by several load-independent indexes and was found to be a consequence of depressed myocardial contractility as well as increased wall stress caused by chamber dilatation without hypertrophy. Unstressed diastolic volume increased without alteration of passive myocardial stiffness. The observation that the zero-pressure intercept of the ESPVR also remained unchanged cautions against the use of extrapolated ESPVRs in this as well as other forms of ventricular dilatation. Contractile reserve to inotropic stimulation is impaired in this form of heart failure as it is in others. Finally, this is the first study to examine the  $MVO_2$ –PVA relation in a dilated cardiomyopathy model. The alterations demonstrated in this relation imply both

increased efficiency of chemomechanical energy transduction and increased oxygen costs of basal metabolism and/or excitation–contraction coupling.

### Appendix

Instantaneous natural strain ( $\epsilon$ ) for the midwall fiber layer was determined from instantaneous LV volume (LVV) and LV mass

$$\epsilon = 0.33 \times \ln(LVV + f \times V_w) / (V_{ref} + c \times V_w) \quad (A1)$$

where  $V_w$  is the ventricular wall volume (1.04 ml/g LV mass) and  $V_{ref}$  is the KCl-arrested diastolic volume (reference volume). The factor  $f$  is the fraction of the ventricular wall volume enclosed by the midwall circumferential fibers at the reference (i.e., diastolic-arrested) state

$$f = \alpha \times (r_{mid}^3 - r_i^3) / V_w \quad (A2)$$

where  $r_{mid} = (r_i + r_o) / 2$ ,  $r_i = (V_{ref} / \alpha)^{1/3}$ ,  $r_o = [(V_{ref} + V_w) / \alpha]^{1/3}$ , and  $\alpha = 4\pi/3$ .

A balanced-force equation for a thick-walled spherical geometry was used to determine instantaneous circumferential stress ( $\sigma$ ) from the LV pressure (LVP) and LVV signals

$$\sigma \text{ (g/cm}^2\text{)} = 1.36 \times LVP \times \beta \times LVV^{2/3} / A_o \quad (A3)$$

where  $A_o$  is the cross-sectional area of the ventricular wall in the equatorial plane and  $\beta = \pi \times [3 / (4\pi)]^{2/3}$ . Rather than use instantaneous LV cross-sectional wall area, the area determined from the diastolic-arrested reference state ( $V_{ref}$ ) was used for all stress calculations

$$A_o = \beta \times [(V_{ref} + V_w)^{2/3} - V_{ref}^{2/3}] \quad (A4)$$

The rationale for this approach is that the force is distributed throughout the same number of muscle fibers at different volumes regardless of the instantaneous cross-sectional wall area.<sup>59</sup>

### Acknowledgments

We gratefully acknowledge the excellent technical assistance of Kenneth Rent and Richard Tunin.

### References

1. Coleman HN, Taylor RR, Pool PE, Whipple GH, Covell JW, Ross J Jr, Braunwald E: Congestive heart failure following chronic tachycardia. *Am Heart J* 1971;81:790–798
2. Chow E, Woodard JC, Farrar DJ: Rapid ventricular pacing in pigs: An experimental model of congestive heart failure. *Am J Physiol* 1990;258:H1603–H1605
3. Armstrong PW, Stopps TP, Ford SE, De Bold AJ: Rapid ventricular pacing in the dog: Pathophysiologic studies of heart failure. *Circulation* 1986;74:1075–1084
4. Wilson JR, Douglas P, Hickey WF, Lanoce V, Ferraro N, Muhammad A, Reichel N: Experimental congestive heart failure produced by rapid ventricular pacing in the dog: Cardiac effects. *Circulation* 1987;75:857–867
5. Howard RJ, Stopps TP, Moe GW, Gotlieb A, Armstrong PW: Recovery from heart failure: Structural and functional analysis in a canine model. *Can J Physiol Pharmacol* 1988;66:1505–1512
6. Riegger AJG, Liebau G: The renin-angiotensin-aldosterone system, antidiuretic hormone and sympathetic nerve activity in an experimental model of congestive heart failure in the dog. *Clin Sci* 1982;62:465–469
7. Moe GW, Stopps TP, Angus C, Forster C, DeBold AJ, Armstrong PW: Alterations in serum sodium in relation to atrial natriuretic factor and other neuroendocrine variables in experimental pacing-induced heart failure. *J Am Coll Cardiol* 1989;13:173–179
8. Schachnow N, Spellman S, Rugin I: Persistent supraventricular tachycardia: Case report with review of the literature. *Circulation* 1954;10:232–236
9. Suga H, Sagawa H: Instantaneous pressure-volume relationship and their ratio in the excised, supported canine left ventricle. *Circ Res* 1974;35:117–126

10. Sunagawa K, Lim KO, Burkoff D, Sagawa K: Microprocessor control of a ventricular volume servo-pump. *Ann Biomed Eng* 1983;10:154-159
11. Burkhoff D, Alexander J, Schipke J: Assessment of Windkessel as a model of aortic input impedance. *Am J Physiol* 1988;255:H742-H753
12. Glower DD, Spratt JA, Snow NK, Kabas JS, Davis JW, Olsen CO, Tyson GS, Sabiston DC Jr, Rankin JS: Linearity of the Frank-Starling relationship in the intact heart: The concept of preload recruitable stroke work. *Circulation* 1985;71:944-1009
13. Kass DA, Maughan WL, Guo ZM, Kono A, Sunagawa K, Sagawa K: Comparative influence of load versus inotropic states on indexes of ventricular contractility: Experimental and theoretical analysis based on pressure-volume relations. *Circulation* 1987;76:1422-1436
14. Suga H: Total mechanical energy of a ventricular model and cardiac oxygen consumption. *Am J Physiol* 1979;236:H498-H505
15. Suga H: Ventricular energetics. *Physiol Rev* 1990;70:247-277
16. Slinker BK, Glantz SA: Multiple linear regression is a useful alternative to traditional analyses of variance. *Am J Physiol* 1988;255:R353-R367
17. Maughan WL, Sunagawa K, Burkhoff D, Graves WL, Hunter WC, Sagawa K: Effect of heart rate on the canine end-systolic pressure-volume relation. *Circulation* 1985;72:654-659
18. Burkhoff D, Yue DT, Oikawa RY, Franz MR, Schaefer J, Sagawa K: Influence of ventricular contractility on non-work-related myocardial oxygen consumption. *Heart Vessels* 1987;3:66-72
19. Suga H, Goto Y, Yasumura Y, Nozawa T, Futaki S, Tanaka N, Uenishi M: O<sub>2</sub> consumption of dog heart under decreased coronary perfusion and propranolol. *Am J Physiol* 1988;254:H292-H303
20. Burkhoff D, Sugiura S, Yue DT, Sagawa K: Contractility-dependent curvilinearity of end-systolic pressure-volume relations. *Am J Physiol* 1987;252:H1218-H1227
21. Kass DA, Beyer R, Lankford E, Heard M, Maughan WL, Sagawa K: Influence of contractile state on curvilinearity of in situ end-systolic pressure-volume relations. *Circulation* 1989;79:167-178
22. McKay RG, Aroesty JM, Heller GV, Royal HD, Warren SE, Grossman W: Assessment of the end-systolic pressure-volume relationship in human beings with the use of a time-varying elastance model. *Circulation* 1986;74:97-104
23. Grossman W, Braunwald E, Mann T, McLaurin LP, Green LH: Contractile state of the left ventricle in man as evaluated from the end-systolic pressure-volume relations. *Circulation* 1977;56:845-852
24. Burkoff D, Flaherty JT, Herskowitz A, Oikawa RY, Sugiura S, Franz MR, Baumgartner WA, Schaefer J, Reitz BA, Sagawa K: In vitro studies of isolated supported human hearts. *Heart Vessels* 1988;4:185-196
25. Alyono D, Ring WS, Crumbley AJ, Schneider JR, O'Connor MJ, Parrish D, Bache RJ, Anderson RW: Global left ventricular contractility in three models of hypertrophy evaluated with E<sub>max</sub>. *J Surg Res* 1984;37:48-54
26. Yin CPF: Ventricular wall stress. *Circulation* 1981;49:829-841
27. Hansen DE, Cahill PD, DeCampi WM, Harrison DC, Derby GC, Mitchell RS, Miller DC: Valvular-ventricular interaction: Importance of the mitral apparatus in canine left ventricular systolic performance. *Circulation* 1986;73:1310-1320
28. Weber KT, Pick R, Silver MA, Moe GW, Janicki JS, Zucker IH, Armstrong PW: Fibrillar collagen and remodeling of dilated canine left ventricle. *Circulation* 1990;82:1387-1401
29. Feldman MD, Alderman JD, Aroesty JM, Royal HD, Ferguson JJ, Owen RM, Grossman W, McKay RG: Depression of systolic and diastolic myocardial reserve during atrial pacing tachycardia in patients with dilated cardiomyopathy. *J Clin Invest* 1988;82:1661-1668
30. Phillips PJ, Gwathmey JK, Feldman MD, Schoen FJ, Grossman W, Morgan JP: Post-extrasystolic potentiation and the force-frequency relationship: Differential augmentation of myocardial contractility in working myocardium from patients with end-stage heart failure. *J Mol Cell Cardiol* 1990;22:99-110
31. Morgan JP, Blinks JR: Intracellular calcium transients in the cat papillary muscle. *Can J Physiol Pharmacol* 1982;60:524-528
32. Shannon RP, Vatner DE, Komamura K, Homcy CJ, Stambler BS, Vatner SF: Impaired  $\beta$ -adrenergic responsiveness in conscious dogs with pacing cardiomyopathy (abstract). *Circulation* 1990;82(suppl III):III-160
33. Fray MJ, Manning D, Wilson JR, Molinoff PB: Alterations in the catalyst of adenylate cyclase and the inhibitory guanine nucleotide regulatory protein in experimental heart failure (abstract). *J Am Coll Cardiol* 1989;13(suppl A):179A
34. Ianussa CD, Montgomery C, Moe G, Armstrong P: Energy status of canine myocardium with congestive heart failure induced by rapid ventricular pacing (abstract). *FASEB J* 1990;4:A281
35. Bache RJ, Arentzen CE, Simon AB, Vrobel TR: Abnormalities in myocardial perfusion during tachycardia pacing in dogs with left ventricular hypertrophy: Metabolic evidence for myocardial ischemia. *Circulation* 1984;69:409-417
36. Fujii AM, Gelpi RJ, Mirsky I, Vatner SF: Systolic and diastolic dysfunction during atrial pacing in conscious dogs with left ventricular hypertrophy. *Circ Res* 1988;62:462-470
37. Hittinger L, Shannon RP, Kohin S, Manders T, Kelley P, Vatner SF: Exercise-induced subendocardial dysfunction in dogs with left ventricular hypertrophy. *Circ Res* 1990;66:329-343
38. Mjos OD: Effect of free fatty acids on myocardial function and oxygen consumption in intact dogs. *J Clin Invest* 1971;50:1386-1389
39. Willebrands AF, van der Veen KJ: Influence of substrate on oxygen consumption of isolated perfused rat heart. *Am J Physiol* 1967;212:1529-1535
40. Drake AJ: Substrate utilization in the myocardium. *Basic Res Cardiol* 1982;77:1-11
41. Kagaya Y, Kanno Y, Takeyama D, Ishide N, Maruyama Y, Takahashi T, Ido T, Takishima T: Effects of long-term pressure overload on regional myocardial glucose and free fatty acid uptake in rats. *Circulation* 1990;81:1353-1361
42. Yonekura Y, Brill AB, Som P, Yamamoto K, Srivastava SC, Iwai J, Elmaleh DR, Livni E, Strauss HW, Goodman MM, Knapp FF Jr: Regional myocardial substrate uptake in hypertensive rats: A quantitative autoradiographic measurement. *Science* 1985;227:1494-1496
43. Burkhoff D, Weiss RG, Schulman SP, Kalil-Filho R, Wannenburg T, Gerstenblith G: Influence of metabolic substrate on myocardial contractile state and metabolism at different coronary flows. *Am J Physiol* 1991;261:H741-H750
44. Allen DG, Kurihara S: The effects of muscle length on intracellular calcium transients in mammalian cardiac muscle. *J Physiol (Lond)* 1982;327:79-94
45. Whalen WJ: Some factors influencing O<sub>2</sub> consumption of isolated heart muscle. *Am J Physiol* 1960;198:1153-1156
46. Yasumura Y, Nozawa T, Futaki S, Tanaka N, Suga H: Minor preload dependence of O<sub>2</sub> consumption of unloaded contraction in dog heart. *Am J Physiol* 1989;256:H1289-H1294
47. Cooper G: Load and length regulation of cardiac energetics. *Annu Rev Physiol* 1990;52:505-522
48. Goto Y, Slinker BK, LeWinter MM: Decreased contractile efficiency and increased nonmechanical energy cost in hyperthyroid rabbit heart: Relation between O<sub>2</sub> consumption and systolic pressure-volume area or force-time integral. *Circ Res* 1990;66:999-1011
49. O'Brien PJ, Ianuzzi CD, Moe GW, Stopps TP, Armstrong PW: Rapid ventricular pacing of dogs to heart failure: Biochemical and physiological studies. *Can J Physiol Pharmacol* 1989;68:34-39
50. LeClercq JF, Swynghedauw B: Myofibrillar ATPase, DNA, and hydroxyproline content of human hypertrophied heart. *Eur J Clin Invest* 1976;6:27-33
51. Alpert NR, Gordon MS: Myofibrillar adenosine triphosphatase activity in congestive heart failure. *Am J Physiol* 1962;202:940-946
52. Mercadier JJ, Bouveret P, Gorza L, Schiaffino S, Clark WA, Zak R, Swynghedauw B, Schartz K: Myosin isoenzymes in normal and hypertrophied human ventricular myocardium. *Circ Res* 1983;53:52-62
53. Lauer B, Van Thiem N, Swynghedauw B: ATPase activity of the cross-linked complex between cardiac myosin subfragment 1 and actin in several models of chronic overloading: A new approach to the biochemistry of contractility. *Circ Res* 1989;64:1106-1115
54. Alpert NR, Mulieri LA: Increased myothermal economy of isometric force generation in compensated cardiac hypertrophy induced by pulmonary artery constriction in the rabbit: A characterization of heat liberation in normal and hypertrophied right ventricular papillary muscles. *Circ Res* 1982;50:491-500
55. Hasenfuss G, Mulieri LA, Blanchard EM, Holubarsch C, Leavitt BJ, Ittleman F, Alpert NR: Energetics of isometric force develop-

- ment in control and volume-overload human myocardium: Comparison with animal species. *Circ Res* 1991;68:836–846
56. Burkhoff D, de Tombe PP, Hunter WC, Kass DA: Contractile strength and mechanical efficiency of left ventricle are enhanced by physiologic afterload. *Am J Physiol* 1991;260:H569–H578
57. Izzi G, Zile MR, Gaasch WH: Myocardial oxygen consumption and the left ventricular pressure-volume area in normal and hypertrophic canine hearts. *Circulation* 1991;84:1384–1392
58. Nozawa T, Yasumura Y, Futaki S, Tanaka N, Igarashi Y, Goto Y, Suga H: Relation between oxygen consumption and pressure-volume area of in situ dog heart. *Am J Physiol* 1987;253:H31–H40
59. Hunter WC, Baan J: The role of wall thickness in the relation between sarcomere dynamics and ventricular dynamics, in Baan J, Arntzenius AC, Yellin EL (eds): *Cardiac Dynamics*. The Hague, Martinus Nijhoff Publishing, 1980, pp 123–134